Research Square

Preprints are preliminary reports that have not undergone peer review.
They should not be considered conclusive, used to inform clinical practice,
or referenced by the media as validated information.

# Clustering of Spin-labeled Drug Fenofibrate in a Lipid Raft-mimicking Bilayer

**Anastasiya N. Atnyukova**
Voevodsky Institute of Chemical Kinetics and Combustion, Russian Academy of Sciences
**Denis S. Baranov**
Voevodsky Institute of Chemical Kinetics and Combustion, Russian Academy of Sciences
**Andrey Yu. Komarovskikh**
Voevodsky Institute of Chemical Kinetics and Combustion, Russian Academy of Sciences
**Sergei A. Dzuba**
dzuba@kinetics.nsc.ru

Voevodsky Institute of Chemical Kinetics and Combustion, Russian Academy of Sciences

**Research Article**

**Keywords:**

**Posted Date:** November 4th, 2026

**DOI:** https://doi.org/10.21203/rs.3.rs-11425551/v1

**License:** This work is licensed under a Creative Commons Attribution 4.0 International License.
Read Full License

**Additional Declarations:** No competing interests reported.

# Abstract

Lipid rafts are domains in biological membranes of relatively ordered (Lo) phase distributed in a relatively disordered (Ld) phase; sterols are an important component of lipid rafts. Fenofibrate is a hypolipidemic drug used to improve lipid profiles, particularly triglyceride and high-density lipoprotein-cholesterol levels. Interaction of fenofibrate with lipid rafts may be of particular interest. Here, spin-labeled analogue of fenofibrate (Feno-SL) in a raft-mimicking lipid bilayer was studied using EPR spectroscopy. The bilayers were formed by a mixture of dioleoyl-glycero-phosphocholine (DOPC), dipalmitoyl-glycero-phosphocholine (DPPC) and cholesterol (Chol). It is found that room-temperature EPR spectra depend only slightly on the presence of Chol, whereas for the frozen state at 200 K EPR spectra demonstrate a pronounced dependence on Chol content. The obtained results are explained by magnetic dipole and spin-exchange interactions occurring at low temperatures in dense clusters of Feno-SL molecules, which are assumed to be present in bilayers. The threshold Chol content at which clustering appears is close to its known value for a given lipid composition required for the formation of lipid rafts at physiological temperatures which suggests that the structure of lipid rafts during membrane freezing differs from the structure of their environment. The observed clustering highlights the important issue of drug accumulation and toxicity in domain-containing biological membranes.


# 1. Introduction

The biological membrane plays a key role in cellular function, separating it from the external environment and enabling a number of important biochemical processes. For most drugs, regardless of their structure, properties, or purpose, binding to lipid membranes is a necessary step in their therapeutic action [1–5]. The interaction of drugs with the lipid bilayer can influence their penetration into the cell, distribution in the body, metabolism and excretion, which is especially important when assessing the toxicity of drugs.

It is known that lipid membranes segregate their components into nano- and microdomains, leading to the formation of a heterogeneous membrane lateral structure; such segregation is supposed to play an important role in the life processes of cells and organisms [6–11]. The resulting inhomogeneities are classified as liquid-ordered phases (Lo) —commonly referred to as lipid rafts—capable of moving within a relatively disordered (Ld) environment. The Lo phase consists predominantly of sterols and saturated lipids, whereas the Ld phase is formed primarily of unsaturated lipids. In addition to these two types, long saturated hydrocarbon chains tend to transition into solid-like gel (g) phase. Phase separation in real biological membranes can be modeled using lipid bilayers, which typically consist of ternary mixtures of a high-melting-point lipid (with fully saturated acyl chains), a low-melting-point lipid (with unsaturated acyl chains), and sterol [10, 11].

The sizes of lipid domains smaller than the resolution limit of standard optical microscopy (200 nm) can be classified as nanodomains [12]. The reviews [12, 13] discuss the possibilities of studying such nanodomains using various experimental methods: Förster resonance energy transfer (FRET) [12–15],

nuclear magnetic resonance (NMR) [16–19], small-angle neutron scattering (SANS) [20] and others. The aim of these studies was to investigate the formation of nanodomains consisting of different types of lipids (zwitterionic and anionic glycerophospholipids, glycosphingolipids, ceramides and others), as well as the influence of chemical, electrostatic and geometric factors and the effects of membrane curvature and asymmetry.

Spin-label EPR is capable to study molecular motion, spatial ordering and some other properties of the molecules in the membranes [11, 21, 22]. When used at low temperatures, spin-label EPR is sensitive to dipole-dipole (d-d) interactions of unpaired electrons of spin labels [23, 24]. Conventional continuous wave (CW) EPR spectra are sensitive to d-d interactions for spin labels located at a distance of less than 1.5 nm from each other, while pulsed EPR techniques such as double electron–electron resonance (DEER, also known as PELDOR) extend the capabilities of EPR to larger distances (up to ~ 8 nm or even more). Both of these methods have been applied to study nanoclusters of spin-labeled molecules of anti-inflammatory drug ibuprofen in the presence of lipid rafts [23, 24]. Experimental approaches to the use of pulsed EPR in the study of nanoclusters of spin-labeled molecules, also in connection with the problem of lipid rafts, were analyzed in a recent review [25].

Ibuprofen is a relatively small molecule with a single benzene ring in its structure, its size is about half that of a cholesterol molecule. In this work, we study the spin-labeled analog of the hypolipidemic drug fenofibrate. The fenofibrate molecule is significantly larger than ibuprofen, it has two separate benzene rings in its structure, and its size is comparable to that of a cholesterol molecule – see Fig. 1.

The hypolipidemic drugs are widely used to correct lipid metabolism disorders. Fenofibrate is a selective agonist of the peroxisome proliferator-activated receptor (PPARα) [26]. In patients with dyslipidaemia, fenofibrate improves the lipid profile, particularly triglyceride and high-density lipoprotein-cholesterol levels [27]. Studying interaction of fenofibrate with lipid rafts—of which cholesterol is an important component—may be of particular interest. It should be noted that in addition to the lipid-lowering effect, fenofibrate may have other therapeutic properties, in particular, its anticancer activity has also been suggested [28, 29].

As model raft-mimicking lipid bilayers, different compositions can be used consisted of high- and low-melting-point lipids, and sterols (see above) [10, 11]. The bilayers studied in this work were prepared of equimolar amounts of 1,2-dioleoyl-sn-glycero-3-phosphocholine (DOPC) and 1,2-dipalmitoyl-sn-glycero-3-phosphocholine (DPPC) with the addition of cholesterol (Chol) in various proportions; that is, the molar ratio in the DOPC/DPPC/Chol mixtures was $(50–x/2):(50–x/2):x$ (with $0 \le x \le 30$). As has been established in studies of these compositions at physiological temperatures using various experimental approaches [11, 30–32], by varying the value of $x$ it is possible to transition at $x \ge \sim 12$ mol% from bilayers without rafts to bilayers containing rafts. (At $x < 12$ mol%, the bilayers consist of Ld and g phases [30]). For this study, it is important to note that low-frequency Raman scattering experiments performed at cryogenic temperatures [33] have shown that fluid-state raft-containing bilayer structures freeze upon cooling.

To enable the use of EPR spectroscopy, a spin-labeled analogue of fenofobrate (Feno-SL) was synthesized [34], see Fig. 1B. Feno-SL molecules have been shown to integrate into biological membranes [34], apparently due to their amphiphilic nature. It should be noted that from a purely structural point of view (see Fig. 1), the addition of a spin label to the original fenofibrate molecule does not change its amphiphilicity.

## 2. Experimental

# 2.1 Materials and Samples

DOPC was from Avanti Polar Lipids, DPPC was from Aladdin Scientific, Chol was from Sigma-Aldrich. Feno-SL was synthesized using the method described earlier [34]. Briefly, the synthesis involves iodination, Sonogashira cross-coupling, and peroxidation steps; the nitroxyl spin label ((4-hydroxy-2,2,6,6-tetramethylpiperidin-1-yl)oxidanil or TEMPOL) is linked to the benzene ring of the parent fenofibrate molecule via an acetylene bridge. The chemical structures of the substances are shown in Fig. 1 (along with parent fenofibrate).

A mixture of DOPC, DPPC and Chol in different molar proportions $(50-x/2):(50-x/2):x$ $(0 \le x \le 30)$ with the addition of Feno-SL at different molar concentrations $\chi$ (equal to either 0.5 mol%, 1 mol% or 2 mol%) was dissolved in chloroform. The solvent was then removed by evaporation in the nitrogen stream. The obtained films were stored under vacuum for 4 h. An excess of phosphate-buffered saline (pH 7.0) was then added at a ratio of 10:1, the sample was mixed, and incubated for 2 hours at room temperature. Samples were centrifuged at 14,000 g for 4 minutes. The final lipid-to-water ratio was 1:3, w/w. This protocol results in the formation of multilamellar vesicles (MLVs). For low-temperature studies, samples were rapidly frozen by immersion in liquid nitrogen.

# 2.2 Measurements

An X-band Bruker ELEXSYS E580 EPR spectrometer was employed, with a Bruker ER 4118X-MD5 dielectric resonator equipped. The modulation amplitude was 0.01 mT, the output microwave power was 200 mW, with its attenuation adjusted to avoid the saturation effects. The sweep time and the spectrometer time constant were 10.49 s and 20.48 ms, respectively. For low-temperature measurements, the resonators were immersed in an Oxford Instruments CF-935 cryostat cooled by a flow of cold nitrogen, the temperature was stabilized by a Bruker ER4131VT temperature controller.

## 3 Results

# 3.1 EPR Spectra at Room Temperature

EPR spectra taken at room temperature ($25^{o}$C) are shown in Fig. 2. These spectra are typical for nitroxide spin labels in biological membranes which experience slow (in the EPR time scale) orientational motion [35]. The spectra are normalized by constant second integral—this normalization equalizes the number

of molecules for samples with different concentrations and volumes. Figure 2A shows that for Chol-free bilayers, EPR spectra depend only slightly on the Feno-SL concentration $\chi$. For Chol-containing bilayers (Fig. 2B) however some dependence on $\chi$ appears: with its increasing, there is some line broadening, which is manifested by a decrease in the intensity of the central line. This broadening can be explained by an increase in the transverse spin relaxation rate $T_2^{-1}$, which affects all three lines equally, but is most noticeable for the central one due to its smallest width. Furthermore, at $\chi$ = 2 mol%, a slight increase in line splitting is observed in Fig. 2B. This increase is typical upon the addition of cholesterol to lipid bilayers for spin labels located in the upper half of the hydrophobic interior of the membrane [11, 21, 22, 36].

It should be noted that the EPR spectra of spin-labeled lipids at room temperature [11, 21, 22] show a much more pronounced dependence on Chol concentration than that shown in Fig. 2 for Feno-SL. For spin-labeled lipids, the main source of this dependence is molecular motion in the surrounding medium; therefore, this difference may be due to the more rigid molecular structure of Feno-SL, which makes it less sensitive to the motion.

## 3.2 EPR Spectra at 200 K

Figure 3 shows the EPR spectra obtained at 200 K. These spectra exhibit a much more pronounced Feno-SL concentration dependence than the spectra at room temperature (cf. Figure 2). In all cases, an increase in the concentration of Feno-SL $\chi$ leads to a broadening of the spectra. For spectra in Fig. 3A, this broadening is easily explained by the emerging of the d-d interaction between the spin labels. (This interaction at room temperature averages out to zero due to its anisotropic nature and rapid molecular motion.) On the presence of Chol (Fig. 3B), the broadening becomes much more noticeable and even changes the overall shape of the spectrum. This effect indicates that the d-d interaction is enhanced in the presence of Chol.

## 3.3 The Effect of Chol Concentration

The influence of Chol content on the spectral shape at 200 K was studied in more detail for the DOPC/DPPC/Chol bilayers with Feno-SL concentration $\chi$ = 2 mol% – see Fig. 4. One can see that the lineshape here experiences two abrupt changes – between 0 and 5 mol% of Chol content and between 15 and 20 mol%.

The change in the EPR lineshape of the Feno-SL for the Chol concentrations $x$ between 0 and 5 mol% can be explained by the possible influence of Chol on the vertical position of the Feno-SL molecule, which would lead to a change in the proton environment of the spin label: if this environment becomes denser, it would lead to a line broadening observed in Fig. 4. A denser proton environment will arise if the Feno-SL molecule moves somewhat deeper into the membrane, which is accompanied by a denser environment of methylene groups. Meanwhile, the change in Fig. 4 in the lineshape Chol concentrations $x$ above 15 mol% may have another cause, which is discussed below.

It was also found that after warming the frozen samples to room temperature, their spectral shape was completely restored – see Fig. S1 in the Supporting Information.

## 3.4 Simulations of the Spectra

In the simulations of the EPR spectra obtained at 200 K, it was assumed that Feno-SL molecules were completely immobilized, and the standard EasySpin program [37] was used. For a Feno-SL concentration of 0.5 mol% in the absence of cholesterol (cf. Figure 3A), the following best-fitted simulation parameters were found: $g_{XX}$ = 2.0096, $g_{YY}$ = 2.0067, $g_{ZZ}$ = 2.0025, $A_{XX}$ = 6.6 G, $A_{YY}$ = 6.0 G, $A_{ZZ}$ = 34.4 G, the initial line shape was Lorentzian with a peak-to-peak line width $\Delta Bp\text{-}p$ = 5.0 G; the results of simulation are shown in Fig. 5A. For Feno-SL concentrations of 1 mol% and 2 mol%, this spectrum in simulations was convoluted with an additional Lorentzian line with $\Delta Bp\text{-}p$ equal to 0.9 G and 1.5 G, respectively. It can be seen that in all the cases there is a good agreement between the experimental and calculated spectra.

Results of simulation of EPR spectra for Chol-containing bilayers presented in Fig. 3B are given in Fig. 5B. The simulation was performed by summing two spectral shapes: one of them represented the narrow triplet, which closely resembles the spectrum for 0.5 mol% of Feno-SL in the absence of Chol (cf. Figure 3A), with parameters $g_{XX}$ = 2.0093, $g_{YY}$ = 2.0068, $g_{ZZ}$ = 2.0026, $A_{XX}$ = 6.4 G, $A_{YY}$ = 6.0 G, $A_{ZZ}$ = 35.8 G, with a peak-to-peak line width $\Delta B_{p-p}$ = 5.4, 6.4, and 6.9 G for 0.5 mol%, 1 mol%, and 2 mol%, respectively; the second was a broad Voigt singlet with $\Delta B_{p-p}$ = 26 G and *g*-factor equal to 2.0069 (for clarity, this singlet line is shown in Fig. S2).

The contribution of the broad line to the total EPR spectrum was 14%, 45%, and 63% at concentrations $\chi$ of 0.5 mol%, 1 mol%, and 2 mol%, respectively. It should be noted that the $A_{ZZ}$ value found, 35.8 G, is somewhat higher than that for bilayers without Chol ($A_{ZZ}$ = 34.4 G, see above). As noted above, this increase of hyperfine splitting in the presence of Chol is characteristic of spin labels located in the upper half of the membrane's hydrophobic interior—this phenomenon has been observed both at physiological temperatures [36] and in the frozen state [38].

# 4 Discussion

The additional broadening in Fig. 5A for Chol-free bilayers as the Feno-SL $\chi$ concentration increases is obviously explained by increasing the d-d interaction between the unpaired electrons of the spin labels. The Lorentzian type for this additional broadening for $\chi$ = 1 mol% and $\chi$ = 2 mol% can be interpreted basing on the assumption of a random spatial distribution of spin labels (in three dimensions). Note that this simple model can be applied in this case only approximately, because in a bilayer structure, the spatial distribution is expected to be closer to two-dimensional. Modeling of spectra for a two-dimensional spatial distribution is easy to achieve [23], but the small values of the observed broadening make a more detailed analysis of the line shape impractical.

The appearance in Fig. 5B of a broad singlet line instead of the original triplet of narrow lines is apparently due to the magnetic spin-exchange interaction between the spins of closely located unpaired

electrons. It is known [39] that for four interacting nitroxide spin labels located in a rigid tetramer at a distance of 0.5–1 nm from each other, a broad singlet-like line indeed appears. This fact suggests that Feno-SL molecules in the studied DOPC/DPPC/Chol bilayers form dense aggregates (clusters), with the minimum number of molecules estimated at four.

Figure S2 shows the EPR spectrum of pure Feno-SL powder, measured at 200 K, along with the broad line used to model the data in Fig. 5B. The line width for the bilayer is noticeably narrower than for the powder, which suggests that its appearance in the bilayer is not the result of a simple release of Feno-SL into a separate phase.

The found *g*-factor of the broad singlet line, equal to 2.0069, is somewhat larger than the isotropic value for the narrow-line triplet, $g_{iso} = (g_{XX} + g_{YY} + g_{ZZ})/3 = 2.0063$. This difference indicates that, during cluster formation, the long axes of the Feno-SL molecules orient themselves approximately parallel to the membrane normal.

For spin exchange to affect EPR spectra, direct contact between molecules is necessary. At room temperature, molecular motion disrupts these direct contacts, and due to the strong dependence of spin exchange interaction on the distances between unpaired electrons, this interaction may become insignificant – which explains the absence of the broad line at room temperature (see Fig. 2B).

To explain the abrupt change in the EPR spectra observed in Fig. 4 at Chol concentrations $x > 15$ mol% (the appearance of broad singlet), it should be noted that at physiological temperatures in bilayers of the composition under study, lipid rafts form at $x > 12$ mol% [11, 30–32] (below 12 mol%, the bilayer phase is a mixture of Ld and g phases [30]). The proximity of these two values suggests that the appearance of the broad singlet may be related to raft formation. This hypothesis also assumes that lipid rafts (the Lo phase) freeze during the freezing process. Note that this assumption is consistent with the results of Raman studies of frozen lipid bilayers of the same composition [33]. Also, this assumption may imply that the frozen g and Lo phases differ from each other (similar to the Ld and Lo phase).

In our previous studies employing DEER spectroscopy of spin-labeled ibuprofen (ibuprofen-SL) in lipid bilayer of the same DOPC/DPPC/Chol raft-mimicking compositions [24], aggregates of these molecules were observed. This aggregation did not result in the appearance of the EPR line narrowed by spin exchange. Some conclusions were also drawn about the structure of these clusters: they consist of 6 molecules arranged in a prismatic configuration. It was also suggested that these clusters form in voids created by subdomains approximately 30 nm in size that were supposed to present in the structure of lipid rafts. Note that the formation of subdomains of approximately similar size was suggested in the studies using FRET – see review [12]. Since the size of the clusters was about 4 nm (this is also the size of the voids between the subdomains)—which is significantly larger than the size of the spin-labeled ibuprofen molecules—these clusters certainly contain lipid molecules in their internal structure.

The results obtained here for Feno-SL show that these relatively large molecules also tend to cluster in lipid bilayers. However, this clustering leads to the formation of denser aggregates compared to

ibuprofen-SL, in which Feno-SL molecules attach to each other in direct contact. Unfortunately, the DEER method is not applicable to the study of dense clusters, with a distance between spin labels less than 1 nm, due to the strong d-d interaction, which makes the DEER signal unobservable.

# 5 Conclusions

The results of this work show that solid-state (ss) CW EPR spectra of clusters of spin-labeled molecules in the membranes can be caused by strong spin exchange effects between the spin labels, which can occur if these molecules are in direct contact with each other. It has previously been shown that for molecules not in close proximity to each other, ss CW EPR provides information on d-d interactions between them [23, 24]. At physiological temperatures, these two types of interaction disappear due to fast molecular motion, which disrupts the direct contact between molecules necessary for strong spin-exchange interaction and averages out the d-d interaction due to its anisotropic nature. Thus, ss CW EPR provides additional opportunities for studying clusters of spin-labeled molecules. Of course, it should be noted that here, compared to physiological temperatures, dynamic information is lost.

In this work, ss CW EPR is used to investigate the clustering of Feno-SL molecules in DOPC/DPPC/Chol bilayers. The results, obtaining as a function of the Chol molar content $x$, showed that clusters of Feno-SL are formed at a threshold value of $x > 15$ mol%. This value is close to that ($x > 12$ mol%) obtained in a study of DOPC/DPPC/Chol bilayers at physiological temperature [11, 30–32] which can be explained by the hypothesis that lipid rafts (Lo phase) formed at physiological temperatures freeze during the freezing process. This hypothesis also assumes that the frozen g phase (existing at physiological temperatures at $x < 12$ mol%) do not differ from the Ld phase.

Clustering of Feno-SL molecules occurs at their threshold concentration of $\chi > 1$ mol% and is observed only in the presence of lipid rafts. The same threshold was also found for spin-labeled ibuprofen [24]. An important difference between these two types of the molecules is that the relatively smaller ibuprofen molecules form well-defined, lipid-mediated clusters [24] whereas the relatively larger spin-labeled fenofibrate molecules form more dense clusters in which the molecules are in direct contact with each other.

Finally, we note that for both ibuprofen and fenofibrate, the observed clustering likely highlights the important issue of drug accumulation and toxicity in domain-containing biological membranes.

# Declarations

The authors declare no competing financial interest.

**Supporting Information**

The Supporting Information is available free of charge at https://

EPR spectra at room temperature before and after freezing to 200 K (Fig. S1)

EPR spectra of Feno-SL powder (Fig. S2)

**Author Contributions**

A.N.A.: sample preparation, measurements, preparing Fig.s, discussion; D.S.B.: synthesis, discussion; A.Y.K.: simulation, discussion; S.A.D.: conceptualization, supervising, writing the paper.

**Funding**

This work was supported by the Russian Science Foundation, project #25-23-00061.

**Data availability**

All data necessary to support the findings of this study are included in this article.

**Ethics approval**

This research did not contain any studies involving animal or human participants, nor did it take place in any private or protected area.

# References

1. A.M. Seddon, D. Casey, R.V. Law, A. Gee, R.H. Templer, O. Ces, Chem. Soc. Rev., 38, 2509–2519 (2009)
2. A.C. Alves, D. Ribeiro, C. Nunes, S. Reis, Biochim. Biophys. Acta – Biomembr. 1858, 2231–2244 (2016)
3. P. Xavier, D. Ciumac, P. Niga, C.M. Johnson, P.M. Claesson, R.A. Campbell, Langmuir, 42, 11024–11034 (2026)
4. E. Salnikov, M. Adélaïde, F. Ramos-Martín, A. Saad, J. Schauer, M. Cremanns, M. Rima, C. Aisenbrey, S. Oueslati, T. Naas, N. Pfennigwerth, S. Gatermann, C. Sarazin, B. Bechinger, N. D'amelio, J. Amer. Chem. Soc. 147, 11199–11215 (2025)
5. T. Yamazaki, K. Kamada, K. Nakabayashi, S. Sotoma, K. Maeda, Y. Yoshida, Langmuir, 41, 22357–22364 (2025)
6. K. Simons, W.L.C. Vaz, Annu. Rev. Bioph. Biomol. Struct. 33, 269–295 (2004)
7. L.J. Pike, J. Lipid Res. 50, S323-S328 (2009)
8. I. Castello-Serrano, F.A. Heberle, B. Diaz-Rohrer, R. Ippolito, C.R. Shurer, P. Lujan, F. Campelo, K.R. Levental, I. Levental, Elife, 12, RP89306 (2024)
9. I. Levental, Nat. Rev. Mol. Cell Biol. 21, 420 – 420 (2020)
10. S. Sonnino, A. Prinetti, Curr. Med. Chem. 20, 4–21 (2013)
11. D. Marsh, Biochim. Biophys. Acta (BBA) – Biomembr. 1788, 2114 – 2123 (2009)

12. M. Cebecauer, M. Amaro, P. Jurkiewicz, M.J. Sarmento, R. Sachl, L. Cwiklik, M. Hof, Chem. Rev. 118, 11259–11297 (2018)
13. J.J. Kinnun, H.L. Scott, D. Bolmatov, C.P. Collier, T.R. Charlton, J. Katsaras, Biophys. J. 122, 931–949 (2023)
14. T.A. Enoki, F.A. Heberle, G.W. Feigenson, Biophys. J. 114, 1921–1935 (2018)
15. E.H. Chaisson, D. Mehta, F.A. Heberle, Biochim. Biophys, Acta (BBA)-Biomembr. 1868, 184505 (2026)
16. S.L. Veatch, I.V. Polozov, K. Gawrisch, S.L. Keller, Biophys. J. 86, 2910–2922 (2004)
17. J. Juhasz, F.J. Sharom, J.H. Davis, Biochim. Biophys. Acta (BBA)-Biomembr. 1788, 2541–2552 (2009)
18. Y. Yano, S. Hanashima, H. Tsuchikawa, T. Yasuda, J.P. Slotte, E. London, M. Murata, Biophys. J. 119, 539–552 (2020)
19. M. Murata, N. Matsumori, M. Kinoshita, E. London, Biophys. Rev. 14, 655–678 (2022)
20. F.A. Heberle, R.S. Petruzielo, J. Pan, P. Drazba, N. Kučerka, R.F. Standaert, G.W. Feigenson, J.J. Katsaras, J. Am. Chem. Soc. 135, 6853–6859 (2013)
21. C. Chachaty, D. Rainteau, C. Wolf, Biophys. J. 88, 4032–4044 (2005)
22. I.V. Ionova, V.A. Livshits, D. Marsh, Biophys. J. 102, 1856–1865 (2012)
23. E.A. Golysheva, A.S. Kashnik, D.S. Baranov, S.A. Dzuba, J. Phys. Chem. B, 129, 650–658 (2025)
24. A.S. Kashnik, D.S. Baranov, S.A. Dzuba, Biochim. Biophys. Acta (BBA) – Biomembr. 1868, 184543 (2026)
25. S.A. Dzuba, Russ. Chem. Rev. 94, RCR5198 (2025)
26. R.S. Rosenson, Expert Rev. Cardiovasc. Ther. 6, 1319–1330 (2008)
27. K. McKeage, G.M. Keating, Drugs, 71, 1917–1946 (2011)
28. Y. Majeed, R. Upadhyay, S. Alhousseiny, T. Taha, A. Musthak, Y. Shaheen, …H. Ding, Sci. Rep. 9, 6316 (2019)
29. L. Peng, N. Zhu, C.J. Zhang, J.P. Long, Y.N. Shi, Q. Yang, Y.-Z. Gong, L. Qin, Life Sci. 401,124541 (2026)
30. J. H. Davis, J. J. Clair, J. Juhasz, Biophys. J. 96, 521–539 (2009)
31. P. Heftberger, B. Kollmitzer, A. A. Rieder, H. Amenitsch, G. Pabst, Biophys. J. 108, 854–862 (2015)
32. Y.V. Zaytseva, I.V. Zaytseva, N.V. Surovtsev. Biochim. Biophys. Acta (BBA)-Biomemb. 1864, 183869 (2022)
33. D.V. Leonov, S.A. Dzuba, N.V. Surovtsev, RSC Adv. 9, 34451–34456 (2019)
34. D.S. Baranov, A.N. Atnyukova, S.V. Komlina, A.S. Kashnik, S.A. Dzuba, Russ. Chem. Bull. 75, 661–666 (2026)
35. D. Marsh, Spin-label Electron Paramagnetic Resonance Spectroscopy. CRC Press 2020: Boca Raton, FL, USA

36. D. Marsh, Proc. Nat. Acad. Sci. 98, 7777–7782 (2001)
37. S. Stoll, A. Schweiger, J. Magn. Reson. 178, 42–55 (2006)
38. W.K. Subczynski, A. Wisniewska, J.J. Yin, J.S. Hyde, A. Kusumi, Biochem. 33, 7670–7681 (1994)
39. H. Sato, V. Kathirvelu, G. Spagnol, S. Rajca, A. Rajca, S.S. Eaton, G.R. Eaton, J. Phys. Chem. B, 12, 2818–2828 (2008)

# Figures

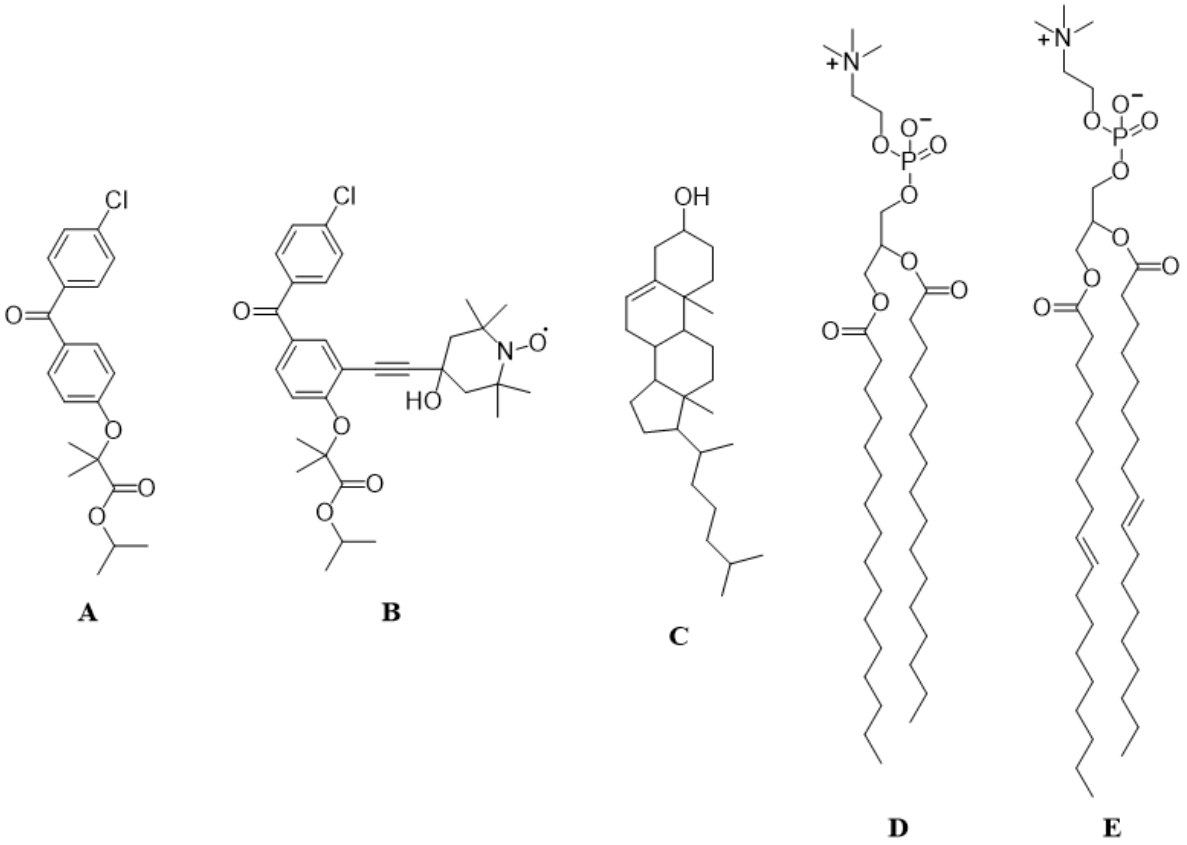



**Figure 1**

Chemical structures: (A) fenofibrate, (B) spin-labeled fenofibrate (Feno-SL), (C) cholesterol (Chol), (D) DPPC, (E) DOPC

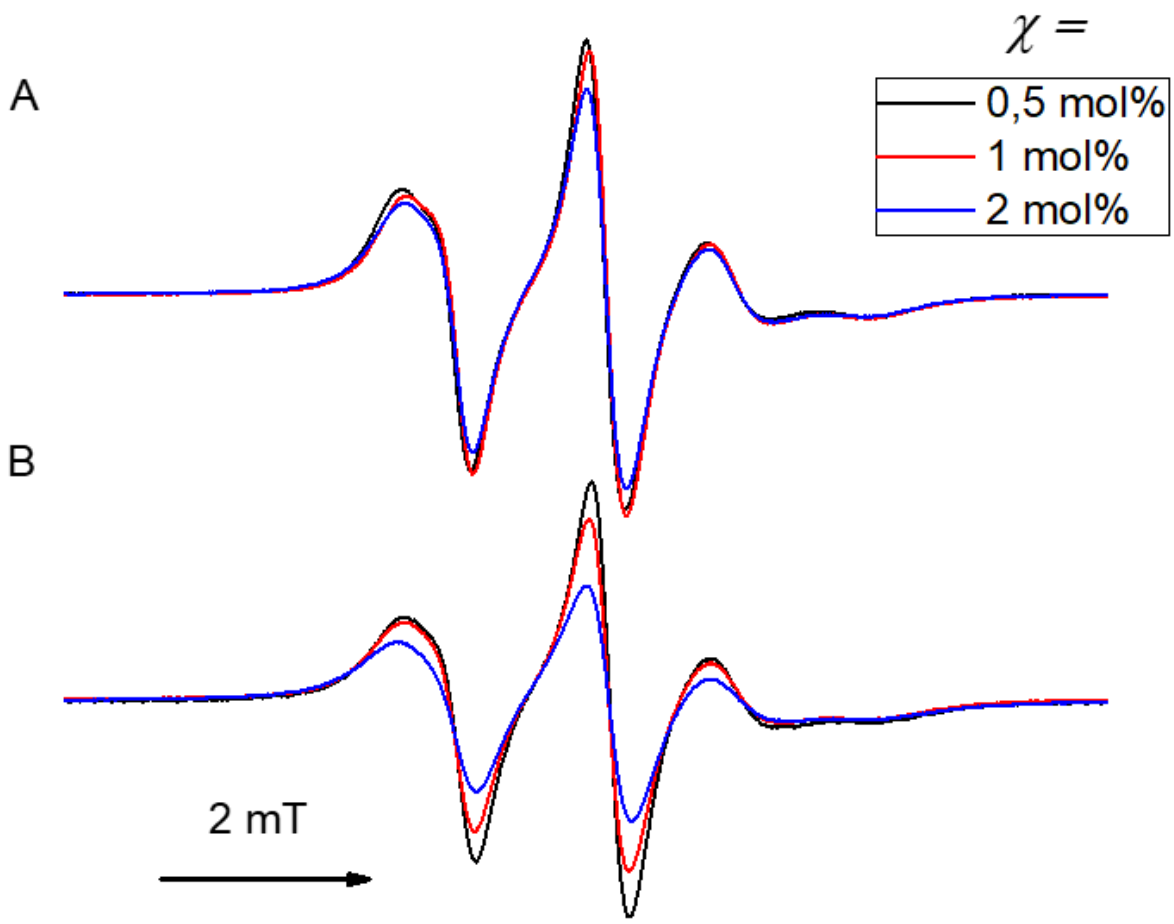



**Figure 2**

EPR spectra at room temperature for Feno-SL at its three different concentrations $\chi$. (A) DOPC/DPPC (50/50) bilayer; and (B) DOPC/DPPC/Chol (35/35/30) bilayer. Spectra are normalized to constant second integral.

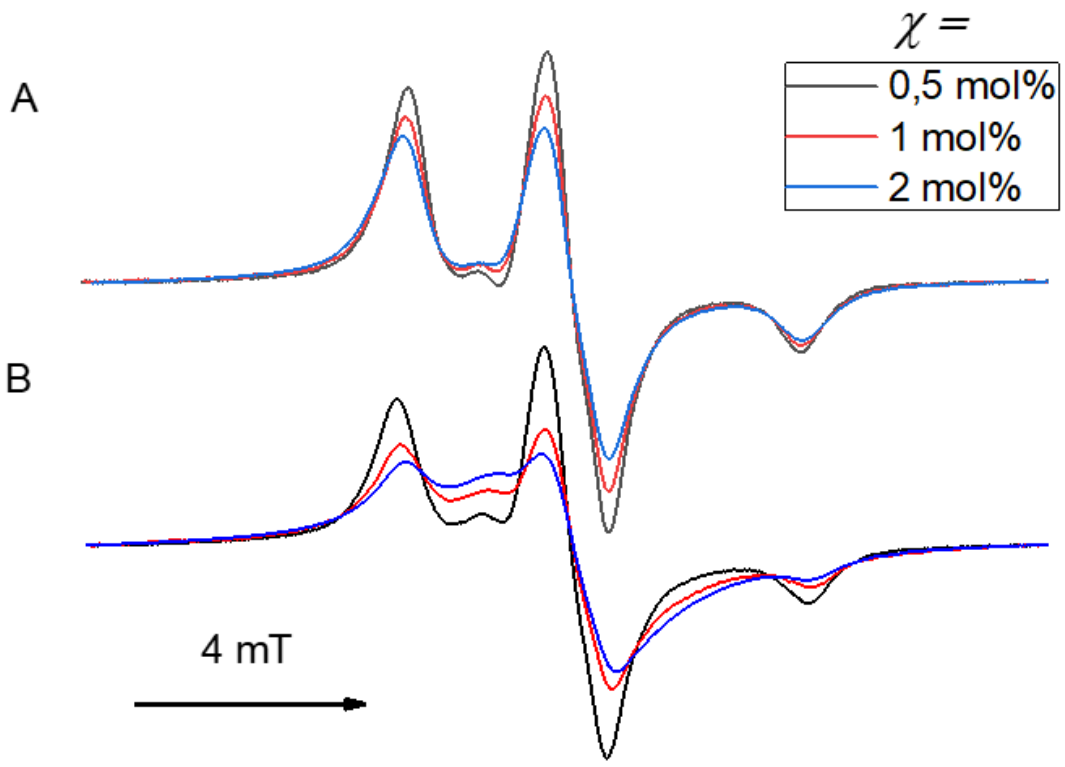



**Figure 3**

EPR spectra at 200 K for Feno-SL at its three different concentrations $\chi$. in (A) DOPC/DPPC (50/50) bilayer; (B) DOPC/DPPC/Chol (35/35/30) bilayer. Spectra are normalized to constant second integral.

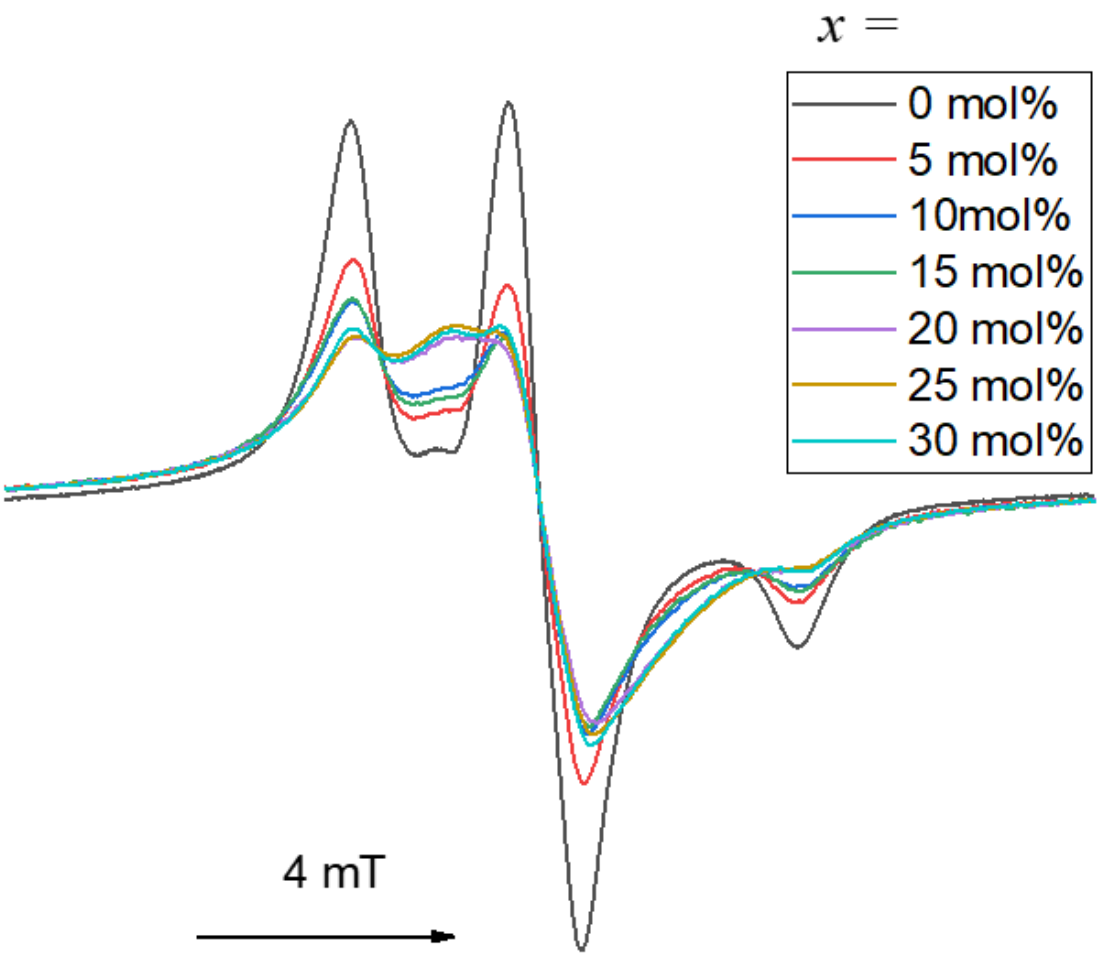



**Figure 4**

EPR spectra at 200 K for Feno-SL with a concentration of $\chi$ = 2 mol% in DOPC/DPPC/Chol bilayers with different Chol contents *x*. Spectra are normalized to constant second integral.

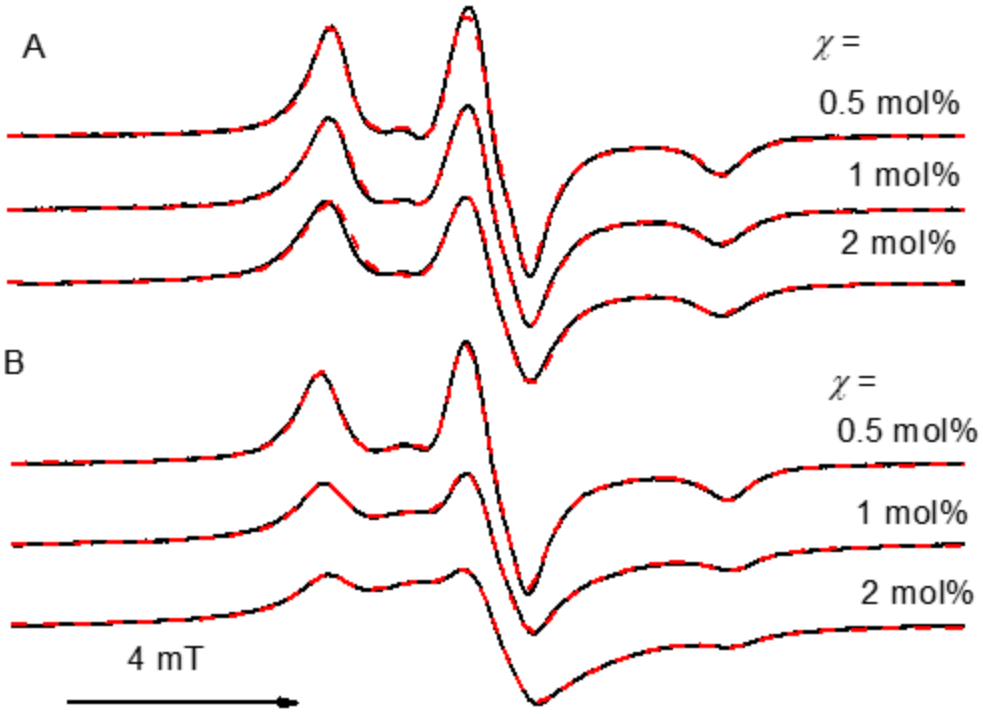



**Figure 5**

EPR spectra at 200 K for Feno-SL of three different concentration $\chi$ in the DOPC/DPPC (50/50) bilayer (A) and DOPC/DPPC/Chol (35/35/30) (B) (solid black lines), as well as the results of their simulation (dashed red lines). The parameters used in the simulation are given in the text.

## Supplementary Files

This is a list of supplementary files associated with this preprint. Click to download.

- SIAMR.docx